ARCHIVES OF METALLURGY AND MATERIALS
Volume 52 2007 Issue 1

K. WIERZBANOWSKI*, A. BACZMAŃSKI*, P. LIPIŃSKI**, A. LODINI***

ELASTO-PLASTIC MODELS OF POLYCRYSTALLINE MATERIAL DEFORMATION AND THEIR APPLICATIONS

MODELE SPRĘŻYSTO-PLASTYCZNE ODKSZTAŁCENIA POLIKRYSZTAŁU I ICH ZASTOSOWANIA

Then elasto-plastic models, used for analysis of polycrystalline material deformation are presented and discussed. Two models are presented in details: the Leffers-Wierzbanowski model and the elasto-plastic self-consistent model, developed by Lipinski, Berveiller and Zaoui. The crystallographic mechanisms of plastic deformation, being the basis of the models, are evoked. The both models have many common elements, they differ, however, in the type of assumed grain-matrix interaction. Some current applications of the decribed models are shown. They are e.g.: prediction of deformation textures, stress-strain curves and distribution of the stored energy as well as the interpretation of residual stress measurement by diffraction technique.

W pracy przedstawiono podstawowe modele typu sprężysto-plastycznego, używane do opisu odkształcenia materiałów polikrystalicznych. Omówiono w szczegółach dwa modele: model Leffersa-Wierzbanowskiego oraz sprężysto-plastyczny model samo-uzgodniony, opracowany przez Lipińskiego, Berveillera i Zaoui. Scharakteryzowano mechanizmy krystalograficzne odkształcenia plastycznego, leżące u podstaw modeli. Oba modele maja wiele wspólnych elementów, różnią się one jednak typem założonego oddziaływania pomiędzy ziarnem i otaczającym go materiałem. Pokazano kilka najczęstszych zastosowań omówionych modeli. Są nimi np.: przewidywanie tekstur odkształcenia, makroskopowych krzywych umocnienia oraz rozkładu energii zgromadzonej w materiale jak również interpretacja dyfrakcyjnych badań naprężeń wewnętrznych.

1. Mechanisms of plastic deformation

Contrary to the elastic deformation, which involves reversible atom displacements, the plastic deformation undergoes by non-reversible mechanisms such as crystallographic slip or (and) mechanical twinning. The both mechanisms are non-reversible, which means that after the release of external forces some permanent deformation stays in the material. Both during the slip and twinning, two parts of crystal (or grain) are sheared one with respect to another. The crystallographic slip is schematically presented in Fig.1. Neighbouring blocs of crystal are relatively displaced. This movement (i.e. slip) occurs on a slip plane (hkl) and along a slip direction [uvw]. Consequently, one defines a slip system [uvw](hkl) and also a family of crystallographically equivalent slip systems <uvw>{hkl}. The slip phenomenon occurs due to a movement of a huge number of dislocations on a slip plane. The dislocation movement, and hence the slip itself, appears in relatively narrow volumes of material, called the slip bands (with an average width h); on the other hand, displaced blocs of crystal (with an average width H) are "inactive" in their volume (Fig. 1).

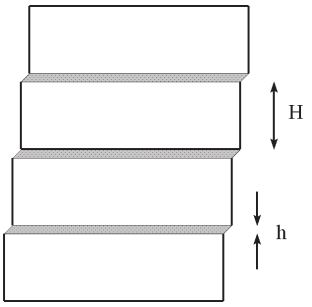

Fig. 1. Slip in a single crystal: blocs of a crystal of an average width H are relatively displaced along the slip plane and slip direction. Regions of an average width h, where slip intensively occurs – are called slip bands; dislocation density is of a few orders of magnitude higher inside slip bands than in other parts of a crystal

Mechanical twinning consists of the shearing movements of atomic planes, which leads to the formation of a crystal region with a crystal lattice being a mirror im-

* FACULTY OF PHYSICS AND APPLIED COMPUTER SCIENCE, AGH UNIVERSITY OF SCIENCE AND TECHNOLOGY, 30-059 KRAKÓW, AL. MICKIEWICZA 30, POLAND
** ECOLE NATIONALE D'INGENIEURS DE METZ, LFM, ILE DU SAULCY, 57045 METZ, FRANCE
*** UNIVERSITE DE REIMS CHAMPAGNE ARDENNE, LACM, 9, BD. DE LA PAIX, 51100 REIMS, FRANCE

age of the original crystal (matrix) – Fig. 2. This newly created crystal region is called *twin*. Let us notice that during a twin formation, all subsequent atom layers of the twin are displaced (by shear movement) with respect to neighbouring ones. "Non-active blocs" do not exit in this case and consequently the shear deformation γ is high. By activation of many slip (or twinning) systems one can obtain any imposed deformation of a crystal. It can be shown that at least five independent shear systems (slip or twinning) are necessary to produce a requested deformation. We will see later that besides of slip also crystal lattice rotation is induced by slip or twinning (Fig. 7).

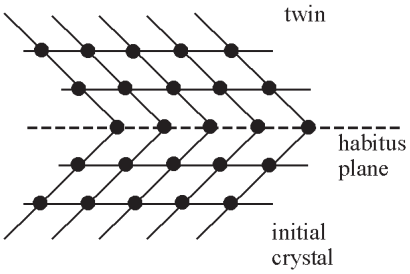

Fig. 2. A twin is created from an original crystal by shearing movements of consecutive atomic layers. A boundary between a matrix and twin crystals is called habitus plane. In analogy to slip, one defines the twinning direction and plane (the latter being parallel to the habitus plane)

Generally, twinning appears in these materials in which a number of independent slip systems is not sufficient to produce an imposed deformation (e.g., in h.c.p. metals or in f.c.c. metals deformed in low temperatures). However, if one considers f.c.c. or b.c.c. metals deformed in room temperature, it is generally sufficient to take into account only slip phenomenon. The exhaustive review of deformation mechanisms in polycrystalline materials can be found in the monograph of Asaro [1].

2. Classification of the models

Mathematical relations describing the elastic deformation (Hooke's law in tensor form) as well as the mechanisms of plastic deformation (slip and twinning) are well known and verified. On the other hand, we dispose of a complete description of the polycrystalline material structure, e.g., by the orientation distribution function (texture), grain boundary size distribution or the distribution of grain boundary orientations and misorientation function. Consequently, one can try to create a deformation model and use it to predict the macroscopic deformation and texture function knowing elementary deformation mechanisms and microstructure description. This would enable to find the transition from the single crystal to the polycrystalline scale. Such the model will describe in a general way the response of a polycrystalline material (elastic and plastic deformation, texture function...) as a result of applying macroscopic forces (expressed by Σ_{ij} tensor) if the initial material microstructure is known. This latter is given by: crystal structure, initial texture, elastic constants, critical stress for slip, initial residual stress, etc.

The basic question, which has to be answered in any model, is: what is the relation between macroscopic variables of the sample (Σ_{ij}, E_{ij}) and analogical microscopic ones (σ_{ij}, ε_{ij}), "seen" by a polycrystalline grain – Fig. 3. Unfortunately, generally it is not possible to find the unknown quantities in an analytical way. That is the reason why we use models.

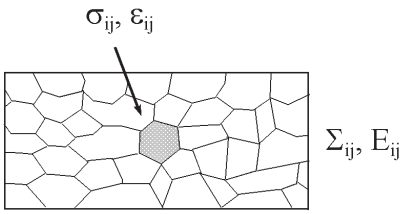

Fig. 3. Macroscopic load Σ_{ij} is applied to a material and as a result a local stress σ_{ij} is seen on a grain level. The sample deformation is E_{ij}, but a local grain deformation is ε_{ij}

It was shown by Hill [2] that a general relation between local and global variables can be written in the form:

$$\dot{\sigma}_{ij} = \dot{\Sigma}_{ij} + L_{ijkl}(\dot{E}_{kl} - \dot{\varepsilon}_{kl}), \tag{1}$$

where L_{ijkl} is an interaction tensor and dot means the time derivative. In the present work we use the convention of the summation on the repeated *lower* indices (for upper indices we apply a classical summation symbol).

A strict calculation of L_{ijkl} tensor is impossible in a general case, hence some simplifying assumptions have to be done. A considerable progress was done by so called self consistent models and many interesting results were found using them [3–7].

Nevertheless, it was found that in many interesting cases the assumption of an isotropic grain-matrix interaction leads to surprisingly good predictions of material properties. In such the case the L_{ijkl} tensor is replaced by a scalar L:

$$\dot{\sigma}_{ij} = \dot{\Sigma}_{ij} + L(\dot{E}_{ij} - \dot{\varepsilon}_{ij}), \tag{2}$$

Some of known models can be reduced to Eq. 2 if L takes appropriate values. For example:
a) $L = 0$ leads to the Sachs model [8] (Sachs, 1928); it is assumed that no interactions between grains appear and consequently a homogeneous stress state results: $\sigma_{ij} = \Sigma_{ij}$,

b) $L \to \infty$ leads to the Taylor model [9] (Taylor, 1938); the basic assumption of the model is a homogeneous plastic deformation in the sample: $\varepsilon_{ij}^{pl} = E_{ij}^{pl}$;
c) $L = \frac{2(7-5\nu)}{15(1-\nu)}\mu$ (where ν is the Poisson coefficient and μ is the shear modulus; $L \cong \mu$ for typical value $\nu \cong 0.3$) is obtained under the assumption of a purely elastic interaction between a grain and the matrix [10] (Kröner, 1961),
d) $L = 2\mu$ leads to Lin model [11]; its basic assumption is: $E_{ij}^{e} + E_{ij}^{pl} = \varepsilon_{ij}^{e} + \varepsilon_{ij}^{pl}$,
e) $L = \alpha\mu$ leads to a compromise description, very close to a real interaction. This is isotropic model with elasto-plastic interaction [3, 12, 13]. The α parameter is called the elasto-plastic accommodation parameter and it describes a partial shape accommodation between grains, caused by some additional local slip. Values of α from the [0.1–0.01] range lead to a good agreement with experimental data. This kind of interaction was used in the Leffers-Wierzbanowski model (LW) [12–17].

Let us recall now some basic quantities, which are common components of any deformation model.

3. Basic quantities in deformation models

Crystallographic slip

* Slip is the elementary mechanism of plastic deformation. It occurs on a crystal plane (hkl) and along a [uvw] direction (situated in this plane). The slip plane is defined by the unit vector **n** (perpendicular to the plane), and slip direction – by the unit vector **m**. A slip system {**m**, **n**} is usually denoted as: [*uvw*](*hkl*). It is very useful to introduce the reference frame connected with the slip system: $\boldsymbol{x}_1^g = \boldsymbol{m}$, $\boldsymbol{x}_3^g = \boldsymbol{n}$ (Fig. 4). The resolved shear stress, decisive for a slip system activation, is easily expressed in this coordinates system: $\tau = \sigma_{13}^g$.

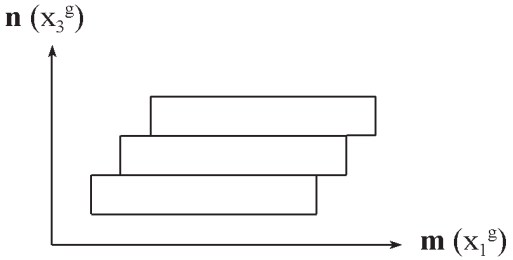

Fig. 4. Displacement of the material during a single slip. The first axis of the ***g*** system is defined by ***m*** vector and the third axis – by ***n*** vector

In a similar way, the glide shear $\Delta\gamma$ produced by a single slip is characterized by only one non-zero component $\Delta e_{13}^{pl(g)} = \Delta\gamma$ of the plastic displacement gradient tensor ($\Delta e_{ij}^{pl(g)}$) (compare Figs. 4 and 5).

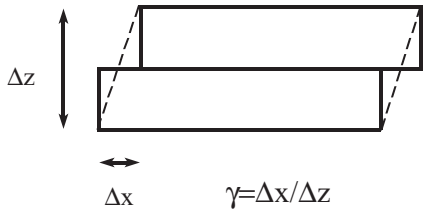

Fig. 5. Definition of the glide shear γ caused by a single slip ($\gamma = \Delta e_{13}^{pl(g)}$)

* The condition for the slip occurrence is:

$$\tau \geqslant \tau_{cr}, \tag{3}$$

i.e., the resolved shear stress ($\tau = \sigma_{13}^g$) has to exceed a critical value τ_{cr} (Schmid law).

The resolved shear stress $\tau = \sigma_{13}^g$ on the slip system {**m**, **n**} is calculated as:

$$\tau = \sigma_{13}^g = a_{1i}a_{3j}\sigma_{ij} = m_i n_j \sigma_{ij}, \tag{4}$$

where σ_{ij} jest the local stress tensor expressed in the sample reference frame – **S** (defined by main symmetry axes of the sample – e.g., rolling, transverse and normal directions in the case of rolling). The coefficients a_{ij} define the transition from the system **S** do **g**. It is practical to define the following quantity:

$$R_{ij} = m_i n_j \tag{5}$$

characterizing the orientation of **g** system with respect to **S**. Finally, we obtain:

$$\tau = R_{ij}\sigma_{ij}. \tag{6}$$

Hardening of slip systems

The slip systems are hardened during deformation, which is visualized in the shape of the stress-strain curve (Fig. 6a). If only one slip system is considered, the hardening curve (τ_{cr} versus γ) in a relatively wide range of deformation has a linear form – Fig. 6b. The physical reason of the hardening is an intensive multiplication of dislocations during plastic deformation. The dislocations are necessary for crystal glide, but if they are in an excessive number – they block each other and this leads to the increasing of critical stress for slip.

Generally, a multi-slip is observed and in such the case the hardening of the system ("*i*") depends on shear glides on other active slip systems ("*j*"):

$$\Delta\tau^i_{cr} = \sum_j H^{ij}\Delta\gamma^j \tag{7}$$

or also:

$$\tau^i_{cr} = \tau_0 + \sum_j H^{ij}\gamma^j. \tag{8}$$

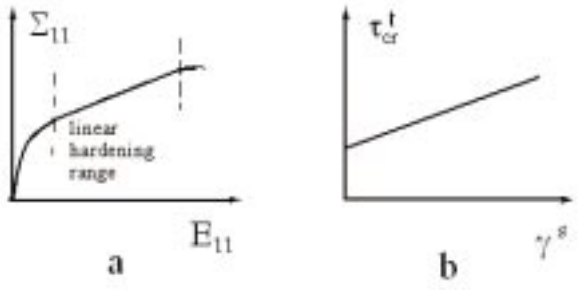

Fig. 6. Hardening curves: a) linear range of stress-strain curve, b) τ_{cr} versus γ (t and s are indices of slip systems) according to linear hardening law

H^{ij} is called the hardening matrix; obviously it is symmetrical. Both theoretical and experimental study show that in the first approximation this matrix contains two types of terms: strong (h_2) and weak (h_1) ones. Their ratio $A = h_2/h_1$ is called the hardening anisotropy coefficient. The terms located on the matrix diagonal (weak terms) describe the self-hardening of slip systems. An exemplary case of a strong term corresponds to a pair of slip systems with perpendicular slip system directions. For the f.c.c. metals (twelve slip systems <110>{111}) the following hardening matrix was found [18]:

$$H^{ij} = h_1 \begin{bmatrix}
1 & & & & & & & & & & & \\
1 & 1 & & & & & & & & & & \\
1 & 1 & 1 & & & & & & & & & \\
1 & A & A & 1 & & & & & & & & \\
A & 1 & A & 1 & 1 & & & & & & & \\
A & A & 1 & 1 & 1 & 1 & & & & & & \\
1 & A & A & 1 & A & A & 1 & & & & & \\
A & 1 & A & A & 1 & A & 1 & 1 & & & & \\
A & A & 1 & A & A & 1 & 1 & 1 & 1 & & & \\
1 & A & A & 1 & A & A & 1 & A & A & 1 & & \\
A & 1 & A & A & 1 & A & A & 1 & A & 1 & 1 & \\
A & A & 1 & A & A & 1 & A & A & 1 & 1 & 1 & 1
\end{bmatrix} \tag{9}$$

Grain deformation and lattice rotation

Let us calculate the deformation and rotation ($\Delta\varepsilon^{pl}_{ij}$ and $\Delta\omega^{pl}_{ij}$), resulting from a glide on one slip system with the shear glide $\Delta\gamma$. In the slip system reference frame ($\boldsymbol{g}$) the displacement gradient tensor has only one non-zero component: $\Delta e^{pl(P)}_{13} = \Delta\gamma$. This tensor after transformation to the sample reference frame (**S**) has the form: $\Delta e^{pl}_{ij} = a'_{i1}a'_{j3}\Delta e^{pl(P)}_{13}$. Taking into account the definition of **S** and **g** systems (Fig. 4) we see that: $a'_{i1} = m_i$ and $a'_{j3} = n_j$ (a'_{ij} define the transformation from $\boldsymbol{g}$ do $\boldsymbol{S}$, while a_{ij} – from **S** do **g**; obviously: $a_{ij} = a'_{ji}$). Finally: $\Delta e^{pl}_{ij} = m_i n_j \Delta\gamma$, or also:

$$\Delta e^{pl}_{ij} = R_{ij}\Delta\gamma. \tag{10}$$

If a multi-slip is occurring, then:

$$\Delta e^{pl}_{ij} = \sum_s R^s_{ij}\Delta\gamma^s, \tag{11}$$

Having Δe^{pl}_{ij}, one finds easily grain deformation and rotation – $\Delta\varepsilon^{pl}_{ij}$ and $\Delta\omega^{pl}_{ij}$ (they are symmetric and anty-symmetric parts of Δe^{pl}_{ij}, respectively):

$$\Delta\varepsilon^{pl}_{ij} = \frac{1}{2}\sum_s (R^s_{ij} + R^s_{ji})\Delta\gamma^s = \sum_s R^s_{(ij)}\Delta\gamma^s \tag{12}$$

$$\Delta\omega^{pl}_{ij} = \frac{1}{2}\sum_s (R^s_{ij} - R^s_{ji})\Delta\gamma^s = \sum_s R^s_{)ij(}\Delta\gamma^s \tag{13}$$

where: $R^s_{(ij)} = \frac{1}{2}(R^s_{ij} + R^s_{ji})$ and $R^s_{)ij(} = \frac{1}{2}(R^s_{ij} - R^s_{ji})$. Let us underline that $\Delta\omega^{pl}_{ij}$ is a rigid body grain rotation produced by slip. If there was not interaction between a grain and the matrix – crystal lattice orientation would not change (see Fig. 7a,b). However, in general a grain does not rotate as a rigid body, because of the constraints imposed by the neighbouring material and a deformation device. As a consequence, some compensating rotation occurs ($\Delta\omega^{latt}_{ij}$) and it changes the grain lattice orientation:

$$\Delta\omega^{latt}_{ij} = -\Delta\omega^{pl}_{ij}. \tag{14}$$

For example, in the tensile test of a single crystal (Fig. 7), the direction defined by a tensile force has to be preserved. This condition imposes a compensating rotation of a crystal, $\Delta\omega^{latt}_{ij}$, which causes the rotation of a lattice.

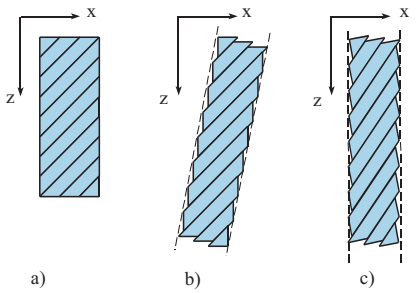

Fig. 7. Tensile test of a crystal along z direction: a) before slip, b) after slip, c) after fulfilment of the condition of z axis preservation (parallel to applied force)

Mascroscopic (sample) deformation

The deformation of the sample is an average over of all grains:

$$E_{ij}^{pl} =< \varepsilon_{ij}^{pl} >= \frac{1}{V_0} \sum_I \varepsilon_{ij}^{pl(I)} V^I, \tag{15}$$

where V^I is the volume of the I-th grain, and V_0 is the sample volume.

Interaction law

Each grain interacts with a neighbouring material. Consequently, a local stress, "seen" by a grain is the superposition of the applied macroscopic load (Σ_{ij}) and reaction stress, resulting from the shape incompatibility (between a grain and the matrix). As it was already mentioned, the local stress is described in general by: $\dot{\sigma}_{ij} = \dot{\Sigma}_{ij} + L_{ijkl}(\dot{E}_{kl} - \dot{\varepsilon}_{kl})$ (Eq. 1). This relation is verified with different precision in various deformation models.

Calculation mode

Calculations are done in incremental way. If we take an example of the rolling deformation and a homogenous material, the applied forces can be approximately presented as:

$$\Sigma_{ij} = \Sigma \begin{bmatrix} 1 & 0 & 0 \\ 0 & 0 & 0 \\ 0 & 0 & -1 \end{bmatrix}, \tag{16}$$

where Σ is the stress "amplitude". In the following step k the amplitude of applied stress tensor is: $\Sigma = \Sigma^0 + (k-1)\Delta\Sigma$.

In each calculation step we find active slip systems. We attribute to each of them elementary glide shear amplitude $\Delta\gamma$ and we calculate the resulting deformation and lattice rotation as well as the modification of reaction stresses (residual stresses). The calculations are stopped in a given step if no more active slip systems are found (due to their hardening). Than we start a new step (k+1), hence we increase the amplitude of the applied stress tensor of $\Delta\Sigma$ and we repeat all the operations described above. We stop the calculations if the macroscopic deformation has attained a preset final value.

4. Self-consistent model

We will give a short review of basic quantities and relations used in the elasto-plastic self-consistent model (SCM).

Ellipsoidal inclusion

The basic assumption of the presented SCM is the representation of an individual grain as a three dimensional ellipsoidal inclusion embedded in an equivalent homogeneous material (Fig. 8).

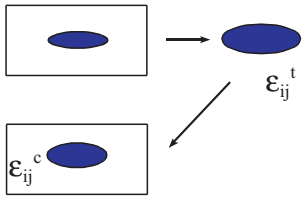

Fig. 8. Problem of ellipsoidal inclusion

Let us assume that we cut out such an inclusion from a homogeneous material (matrix) and we take it outside. Next, we impose a change of its form, which is described by ε_{ij}^t tensor. In the following step, we insert back the inclusion to the hole in the matrix; its final deformation is ε_{ij}^c. The relation between ε_{ij}^c and ε_{ij}^t was derived by Eshelby [19], and is given by means of the S_{ijkl} tensor:

$$\varepsilon_{ij}^c = S_{ijkl}\varepsilon_{kl}^t. \tag{17}$$

The S_{ijkl} tensor is of basic importance, because it characterizes the interaction of a grain with the sample (matrix).

Description of polycrystal

Polycrystalline grains are presented as ellipsoidal inclusions.

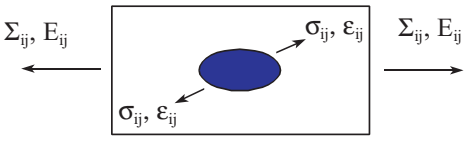

Fig. 9. Polycrystalline grain as an ellipsoidal inclusion

The basic problem in deformation modelling is to find the relation between local (σ_{ij}, ε_{ij}) and global characteristics (Σ_{ij} et E_{ij}). This relation is less direct in the

case of SCM than, e.g., in the case of LW model. In the following text we present the calculation mode used in the elasto-plastic SCM, based on the scheme proposed by Lipinski and Berveiller [4].

Elastic constants and tangent moduli

In the elastic range a general form of the Hook's law is used:

$$\Sigma_{ij} = C_{ijkl} E_{kl} \text{ and } \sigma^I_{ij} = c^I_{ijkl} \varepsilon^I_{kl}, \tag{18}$$

where C_{ijkl} and c^I_{ijkl} are stiffness tensors of the sample and the I-th grain, respectively, and E_{kl} and ε^I_{kl} are corresponding deformation tensors. In the elasto-plastic deformation range we use analogical relations, but concerning the stress and strain increments:

$$\Delta\Sigma_{ij} = L_{ijkl} \Delta E_{kl} \text{ and } \Delta\sigma^I_{ij} = l^I_{ijkl} \Delta\varepsilon^I_{kl}, \tag{19}$$

where L_{ijkl} and l^I_{ijkl} are so called tangent modulus of the sample and the I-th grain, respectively (let us recall that the summation convention does not concern the upper repeated indices). The tangent modulus tensor of a grain, l^I_{ijkl}, can be calculated if active slip systems and corresponding glide shears are known for this grain.

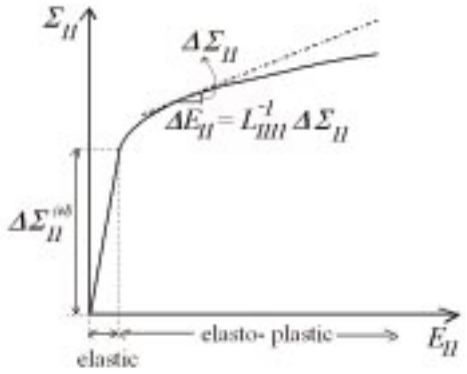

Fig. 10. Determination of $(L^{-1})_{1111}$ from the stress-strain curve

The sample tangent modulus, L_{ijkl}, is obtained by appropriate averaging of grain tangent moduli (Eq. 32). If the elastic deformation range is considered then: $L_{ijkl} = C_{ijkl}$ and $l^I_{ijkl} = c^I_{ijkl}$. The single crystal elastic properties are known in general and the same properties for the sample can be calculated using some hypothesis concerning grain-grain interactions (e.g. models presented in [10, 20, 21]. In the elasto-plastic range tangent moduli change with deformation and their values must be continuously calculated. Some components of the L_{ijkl} tensor have a direct experimental interpretation. For example the $(L^{-1})_{1111}$ component can be determined from the stress-strain curve – Fig. 10.

Interaction between a grain and its environment

Interaction between a grain and the matrix can be directly calculated using the Eshelby tensor S_{ijkl} (eq.17). However, in the present paper the calculation scheme developed by Lipinski and Berveiller [4] is used.

According to Eq. 19, the local stress in the elasto-plastic range is:

$$\dot{\sigma}_{ij}(\mathbf{r}) = l_{ijkl}(\mathbf{r}) \dot{\varepsilon}_{kl}(\mathbf{r}) \tag{20}$$

where $l_{ijkl}(\mathbf{r})$ is the local tangent modulus tensor ("I" grain index was omitted). This tensor can be also written as:

$$l_{ijkl}(\mathbf{r}) = L_{ijkl} + \delta\, l_{ijkl}(\mathbf{r}) \tag{21}$$

where $\delta\, l_{ijkl}(\mathbf{r})$ is a variable part depending on position in the material (let us note that it is simply the difference between the local and global tangent moduli: $\delta\, l_{ijkl}(\mathbf{r}) = l_{ijkl}(\mathbf{r}) - L_{ijkl}$. Introducing the modified Green tensor, $\Gamma_{ijkl}\,(\mathbf{r} - \mathbf{r}')$, the local deformation can be expressed as [4, 22]:

$$\dot{\varepsilon}_{ij}(\mathbf{r}) = \dot{E}_{ij} + \int_V \Gamma_{ijkl}(\mathbf{r} - \mathbf{r}')\delta\, l_{klmn}(\mathbf{r}')\, \dot{\varepsilon}_{mn}(\mathbf{r}')\; dV' \tag{22}$$

Physical sense of the above equation is explained in Fig. 11a: The local deformation in the point $\mathbf{r}$ depends on deformation $\varepsilon_{mn}(\mathbf{r}')$ and $\delta\, l_{klmn}(\mathbf{r}')$ tensors in any other point $\mathbf{r}'$; these quantities are linked by the $\Gamma_{ijkl}\,(\mathbf{r} - \mathbf{r}')$ tensor.

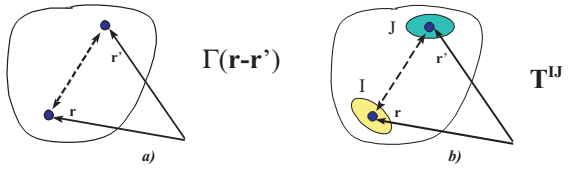

Fig. 11. a) Deformation in the point r depends on deformation in any other point $\mathbf{r}'$ and is described by the Green's tensor, b) interaction between inclusions "I" and "J" is described by T^{IJ} tensor

Deformation in the inclusion (grain) "I" can be expressed as [4]:

$$\dot{\varepsilon}_{ij} = \dot{E}_{ij} + \sum_{J=1}^{N} T^{IJ}_{ijkl}\; \delta\, l^J_{klmn} \dot{\varepsilon}^J_{mn} \tag{23}$$

where T^{IJ}_{ijkl} tensor describes the interaction between inclusions "I" and "J" and N is total number of them. Let us note that the above relation is a discretized form of Eq. 22, if:

$$T^{IJ}_{ijkl} = \frac{1}{V_I} \int_{V_I} \int_{V_J} \Gamma_{ijkl}(r - r')dV dV'. \tag{24}$$

We assume that $\delta\ l^J_{klmn}$ and ε^J_{mn} are homogeneous inside each inclusion (grain). The interaction between inclusions "I" and "J" is schematically shown in Fig. 11b. We will see later that the tensor T^{II}_{ijkl} is a very important quantity, because it describes the interaction of the I-th inclusion with its environment. This tensor is used in one-site approach which, which is applied in this work.

Concentration tensors

We return now to the relations between local and global variables. Let us assume that there exist concentration tensors for deformation (A^I_{ijkl}) and for stress (B^I_{ijkl}), which enable the calculation of local variables from the global ones:

$$\dot{\varepsilon}^I_{ij} = A^I_{ijkl}\dot{E}_{kl} \tag{25}$$

$$\dot{\sigma}^I_{ij} = B^I_{ijkl}\dot{\Sigma}_{kl}. \tag{26}$$

We will consider separately the elastic and elasto-plastic ranges of deformation.

a) *Elastic deformation range*:

It can be derived [23] that using the T^{II}_{ijkl} tensor (one-site approach) and the Hooke's law (Eq. 18) one obtains:

$$[(A^I)^{-1}]_{ijkl} = I_{ijkl} - T^{II}_{ijmn}(c^I_{mnkl} - C_{mnkl}), \tag{27}$$

where I_{ijkl} is the unit tensor. The macroscopic (sample) stiffness tensor, C_{ijkl}, appearing in the above equation is expressed as:

$$C_{ijkl} = \sum_{I=1}^{N} f^I\ c^I_{ijmn}A^I_{mnkl}, \tag{28}$$

where f^I is the volume share of the grain "I". It is clear from the above equations that A^I_{ijkl} and C_{ijkl} tensors depend one on another. Consequently, they are determined using a self-consistent calculation procedure. Once the A^I_{ijkl} tensor is calculated, the second concentration tensor can be found using the Hooke's law:

$$B^I_{ijkl} = c^I_{ijmn}A^I_{mnop}(C^{-1})_{opkl} \tag{29}$$

b) *Elasto-plastic deformation range*:

We obtain analogous results as above if C_{ijkl} tensor is replaced by L_{ijkl} and c^I_{ijmn} – by l^I_{ijmn} one. Moreover, Eq. 19 or its equivalent form:

$$\dot{\Sigma}_{ij} = L_{ijkl}\dot{E}_{kl} \text{ and } \dot{\sigma}^I_{ij} = l^I_{ijkl}\dot{\varepsilon}^I_{kl}, \tag{30}$$

has to be used instead of the Hooke's law.

As a result, the concentration tensor is:

$$[(A^I)^{-1}]_{ijkl} = I_{ijkl} - T^{II}_{ijmn}(l^I_{mnkl} - L_{mnkl}) \tag{31}$$

with the sample tangent modulus tensor defined as:

$$L_{ijkl} = \sum_{I=1}^{N} f^I\ l^I_{ijmn}A^I_{mnkl}. \tag{32}$$

The concentration tensor for stress is:

$$B^I_{ijkl} = l^I_{ijmn}A^I_{mnop}(L^{-1})_{opkl}. \tag{33}$$

Criteria of slip system selection

Three criteria of slip system selection were examined:

a) a set of systems minimizing the plastic work is chosen (MW criterion),
b) five systems, which exceed maximally the Schmid's criterion are selected (ML criterion),
c) a series of systems selected step by step is active; the shear glide is very small and constant for each of them and each active system exceeds maximally the Schmid's law in a given moment (LW criterion).

In the course of many calculations it was found that the three above criteria lead to rather similar deformation and texture predictions.

5. Exemplary results obtained with the models

The models can be used for prediction of important material characteristics, e.g.:

– crystallographic texture,
– hardening curves (e.g., stress-strain curves),
– residual stresses,
– plastic flow surfaces,
– dislocation density and stored energy.

Exemplary comparison of predicted and experimental rolling textures for low carbon steel is shown in Fig. 12. The <110>{111} slip systems and SCM were used. The qualitative agreement between predicted and experimental textures is very good.

Another important characteristic is the stress-strain curve – Fig. 13. Tensile and compression tests were considered. During each of them the increase of loading force was stopped many times for several minutes. The points obtained in such a way correspond to equilibrium condition or to infinitely slow deformation. They agree very well with the model predictions (SCM), which is not rate sensitive (not visco-plastic) but elasto-plastic one.

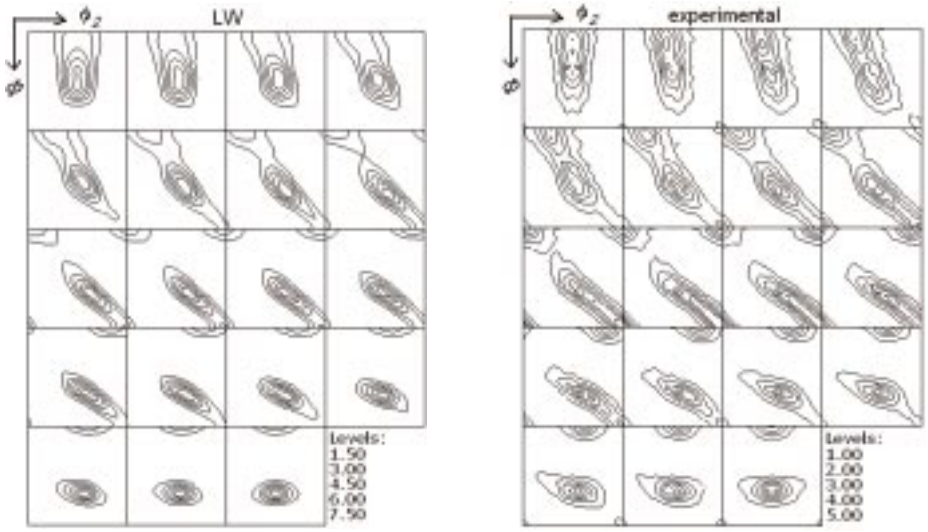

Fig. 12. Comparison of predicted (SCM, LW criterion, E_{eq} = 60%) and measured orientation distribution function for cold rolled low carbon steel, E_{eq} = 105%); φ_2 =const sections are shown

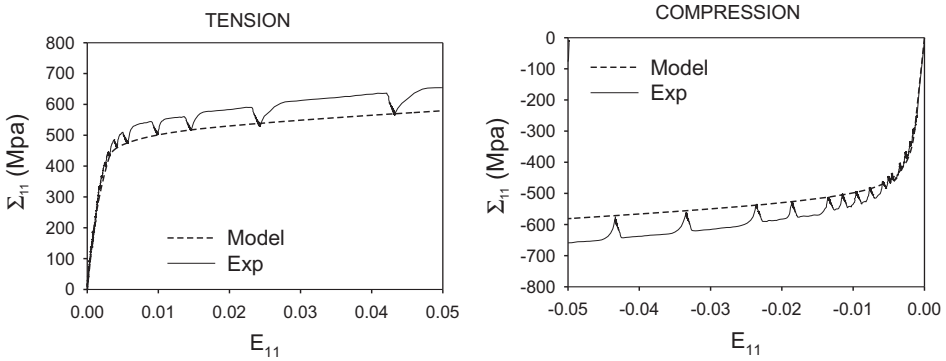

Fig. 13. Predicted stress-strain curves in tension and compression tests for low carbon steel (broken curves) and experimental curves obtained during fast deformation (solid lines). The increase of external load was stopped several times during experiment and the equilibrium points (corresponding to infinitely slow deformation) agree perfectly with the predictions of elasto-plastic SCM.

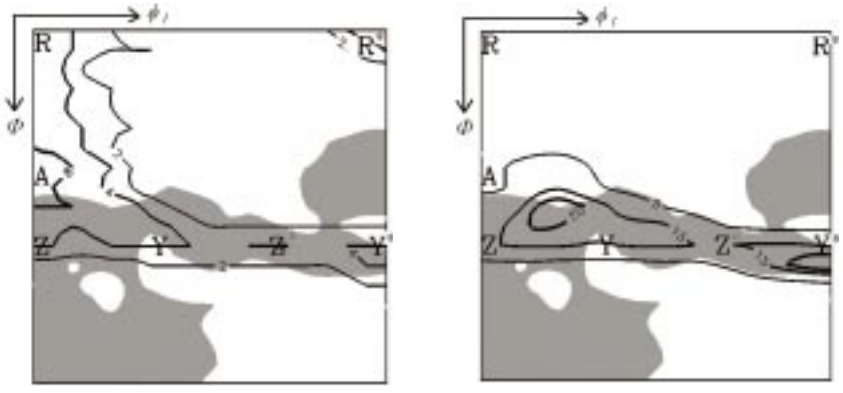

Fig. 14. Texture of low carbon steel (contours) and its relation to the stored energy: a) rolling texture, b) recrystallization texture. The maximum of the stored energy distribution (black area), predicted by SCM is shown; φ_2 = 45° section is shown

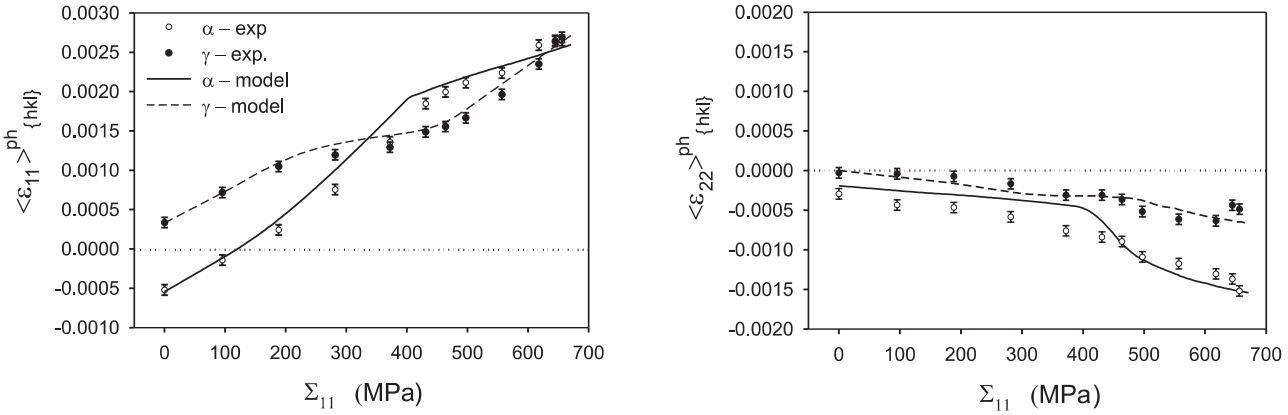

Fig. 15. Measured and calculated (SCM) crystal lattice strain in α and γ phases of austeno-ferritic steel. The results were obtained using neutron diffraction and in situ tensile test

The third example, we present here, is the prediction of the stored energy distribution (proportional to the dislocation density) versus crystal orientation in aspect of texture change during recrystallization – Fig. 14. The low carbon steel was considered and the predictions were obtained using SCM. In the same figure the rolling and recrystallization textures of low carbon steel are shown. It is visible that the γ texture fibre (horizontal one) is reinforced and the α fibre (vertical one) is reduced during annealing. We observe that the model predicts the high values of the stored energy for the γ fibre. It is generally accepted that recrystallization nuclei form in grains with high stored energy and this could explain the observed texture change [24].

Finally, let us mention about the application of deformation models in the field of residual stress analysis – Fig. 15. Two strain components induced by the external force in each phase of the austeno-ferritic steel were measured and calculated using SCM. The neutron diffraction was used for strain measurement. A very good agreement between prediction and experiment confirms the model and its parameters.

6. Conclusions

The presented models of elasto-plastic deformation are useful tools for the study of mechanical properties of polycrystalline materials. They enable predictions of macroscopic material properties (e.g., texture, stress-strain curve, plastic flow surfaces, dislocation density, final state of residual stress) basing on its micro-structural characteristics (crystallography of slip systems, hardening law, initial residual stress state, etc.). Such the models are precious tools for technologists searching for optimal material properties.

Acknowledgements

This work was supported by the Polish Ministry of Science and Higher Education (MNiSW) and by the European Network of Excellence: Complex Metallic Alloys (EU 6-th Frame Program).

REFERENCES

[1] R. J. Asaro, Micromechanics of Crystals and Polycrystals, Adv. in Appl. Mech. **23**, 1-115 (1983).
[2] R. Hill, Continuum Micro-Mechanics of Elastoplastic Polycrystals, J. Mech. Phys. Solids **13**, 89 (1965).
[3] M. Berveiller, A. Zaoui, An Extension of the self-consistent scheme to plastically flowing polycrystals, J. Mech. Phys. Solids **26**, 325 (1979).
[4] P. Lipinski, M. Berveiler, Elastoplasticity of micro-inhomogeneous metals at large strains, Int. Journal of Plasticity **5**, 149 (1989).
[5] A. Molinari, G. R. Canova, S. Ahzi, A Self Consistent Approach of the Large Deformation Polycrystal Viscoplasticity, Acta Met. **35**, 2983 (1987).
[6] R. J. Asaro, A. Needleman, Acta Mater. **33**, 923-953 (1985).
[7] R. A. Lebensohn, C. N. Tome, Acta Mater. **41**, 2611 (1993).
[8] G. Sachs, On the Derivation of a Condition of Flow, Z. Verein. Deutsch. Ing. **72**, 734 (1928).
[9] G. I. Taylor, Plastic Strain of Metals, J. Inst. Met. **62**, 307 (1938).
[10] E. Kröner, Zur plastischen Verformung des Vielkristalls, Acta Met. **9**, 155 (1961).
[11] T. H. Lin, Analysis of Elastic and Plastic Strains of a FCC Crystal, J. Mech. Phys. Solids **5**, 143 (1957).
[12] K. Wierzbanowski, Some Result of a Theoretical Study of Plastic Deformation and Texture Formation in Polycrystals, Zesz. Nauk. Akademii Górniczo-Hutniczej, Nr 1132, Fizyka, zeszyt 12, Kraków (1987).

[13] K. Wierzbanowski, Generalized Computer Program for Texture Simulation, Arch. Hutn. **27**, 189 (1982).
[14] T. Leffers, Computer Simulation of the Plastic Deformation in Face-Centred Cubic polycrystals and the Rolling Texture Derived, phys. stat. sol. **25**, 337 (1968).
[15] K. Wierzbanowski, J. Jasieński, Some Comments on Sachs and Taylor Type Deformation, Scripta Met. **15**, 585 (1981).
[16] K. Wierzbanowski, Computer Simulation of Rolling Texture Formation in H.C.P. and Orthorhombic Metals, Scripta Met. **13**, 795 (1979).
[17] K. Wierzbanowski, Z. Jasieński, Some Results of Examination of Rolling Texture Heterogeneity, Scripta Met., **16**, 653 (1982).
[18] P. Franciosi, M. Berveiller, A. Zaoui, Latent Hardening in Copper and Aluminium Single Crystals, Acta Met. **28**, 273 (1980).
[19] J. D. Eshelby, The Determination of the Elastic Field of an Ellipsoidal Inclusion and Related Problems, Proc. Roy. Soc. London, **A241**, 376 (1957).
[20] A. Reuss, Berechnung der Fliessgrenze von Mischkristallen auf Grund der Plastizitätsbedingung für Einkristalle, Z. Angew. Math. Mech. **9**, 49 (1929).
[21] W. Voigt, Lehrbuch der Kristallphysik, Leipzig, BG Teubner Verlag (1928).
[22] T. Mura, Micromechanics of Defects in Solids, Kluwer Academic Publischer, Dordrecht/Boston/London 1993 (first edition 1982).
[23] A. Baczmanski, Habilitation Thesis, Faculty of Physics and Applied Computer Sciences, AGH UST, Kraków, Poland (2005).
[24] K. Wierzbanowski et al., Deformation Characteristics Important for Nucleation Process. Case of Low-Carbon Steels, Arch. of Metall. **44**, 183 (1999).

Received: 10 September 2006.